European Journal of Medicinal Chemistry 74 (2014) 135–144

Contents lists available at ScienceDirect

European Journal of Medicinal Chemistry

journal homepage: http://www.elsevier.com/locate/ejmech

Original article

Novel lung adenocarcinoma and nuclear factor-kappa B (NF-κB) inhibitors: Synthesis and evaluation of lantadene congeners

Sharad Kumar Suthar [a], Hong L. Boon [b], Manu Sharma [a,*]

[a] Department of Pharmacy, Jaypee University of Information Technology, Waknaghat 173234, India
[b] Cancer Research Initiative Foundation, Drug Discovery Laboratory, 12A Jalan TP5, Taman Perindustrian UEP, 47600 Subang Jaya, Selangor Darul Ehsan, Malaysia

ARTICLE INFO

Article history:
Received 26 August 2013
Received in revised form
24 December 2013
Accepted 26 December 2013
Available online 8 January 2014

Keywords:
Tumor necrosis factor-alpha
Nuclear factor-kappa B
Inhibitor of nuclear factor-kappa B kinase β
A549 lung cancer cells
Lantadene congeners

ABSTRACT

The C-3, C-17 and C-22 congeners of pentacyclic triterpenoids reduced lantadene A (**3**), B (**4**) and 22β-hydroxyoleanolic acid (**5**) were synthesized and were tested *in vitro* for their NF-κB and IKKβ inhibitory potencies and cytotoxicity against A549 lung cancer cells. The lead congeners **12** and **13** showed IC_{50} of 0.56 and 0.42 μmol, respectively against TNF-α induced activation of NF-κB. The congeners **12** and **13** exhibited inhibition of IKKβ in a single-digit micromolar dose and at the same time, **12** and **13** showed marked cytotoxicity against A549 lung cancer cells with IC_{50} of 0.12 and 0.08 μmol, respectively. The lead ester congeners were stable in the acidic pH, while hydrolyzed readily in the human blood plasma to release the active parent moieties.

1. Introduction

Transcription factor nuclear factor-kappa B (NF-κB) influences the gene expression events that impact a large number of biological processes including immune response, cell survival, differentiation, and proliferation [1]. Recent studies have revealed key roles of NF-κB signaling in pathological conditions such as oncogenesis and inflammation. NF-κB is commonly over-expressed and constitutively activated in different types of hematologic cancers and solid tumors [2]. Constitutive activation of NF-κB promotes tumor proliferation, invasion, and metastasis. Moreover, NF-κB activation allows malignant cells to escape apoptosis and therefore, contributes to the development of radiation and chemotherapy resistance in cancer cells [3,4]. Many chemotherapeutic agent has been found to activate NF-κB via various approaches, leading to chemo-resistance and subsequent failure of chemotherapy [5,6]. There are number of evidences which suggest that the inhibition of NF-κB activation can prevent tumor resistance to chemotherapeutic agents, shift the death-survival balance toward apoptosis, and improve the efficacy of current chemotherapeutic regimens [5]. Therefore, designing of NF-κB inhibitors is an interesting approach to develop the new cancer therapeutics.

In last two decades, number of compounds has been reported to inhibit NF-κB by interacting with key molecules in the signaling pathway [7]. Recently, pentacyclic triterpenoids lantadene A (**1**) and B (**2**) isolated from the leaves of weed *Lantana camara* L. (Verbenaceae) have attracted a lot of interest because of their anticancer properties [8–11]. These compounds along with reduced lantadene A (**3**), reduced lantadene B (**4**), and 22β-hydroxyoleanonic acid (**5**) showed potent cytotoxic effects in antitumor screening launched by the National Cancer Institute, USA [12] and were found to be potent inhibitors of NF-κB [8,9,13]. The promising results obtained with a diverse but limited series of target compounds have prompted us to further explore the new analogs of lantadenes. Based on the SAR information obtained in our previous work, we have synthesized new lantadene analogs with different substituents at C-3 position of ring A, C-17 and C-22 positions of the ring D and E, respectively of lantadenes. These congeners were evaluated for their *in vitro* anticancer activity and TNF-α-induced NF-κB activation against lung adenocarcinoma cell line A549. The most active compounds were evaluated *in vitro* for their inhibitory potency against the recombinant IKKβ in a non-radioisotope Kinase-Glo Luminescent Kinase Assays. The most active ester congeners were also studied for their stability in the acidic pH and hydrolysis in the human blood plasma. The lead congener was further docked with the crystal structure of IKKβ to predict the possible binding mode of the congener.

* Corresponding author. Tel.: +91 1792 239219; fax: +91 1792 245362.
E-mail address: lantadene@hotmail.com (M. Sharma).

0223-5234/$ – see front matter © 2014 Elsevier Masson SAS. All rights reserved.
http://dx.doi.org/10.1016/j.ejmech.2013.12.052

2. Results and discussion

2.1. Chemistry

The sequence of steps involved in synthesis of lantadene congeners (**3**–**22**) is summarized in Schemes 1 and 2. Pentacyclic triterpenoid lantadene A (**1**) and B (**2**) were isolated from the leaves of weed *L. camara* Linn. The isolated compounds **1** and **2** differ only in arrangement of atoms in side chain with *E* conformation present in the side of **1**, while side chain of compound **2** possessed *Z* conformation. The isolated compounds **1** and **2** were selectively reduced into corresponding compounds **3** and **4** in 87.60–89.88% yield, using sodium borohydride as reducing agent and methanol (MeOH)–tetrahydrofuran (THF) mixture as solvent. The compound **5** was synthesized in 76.47% yield by alkali hydrolysis of **1** and **2** using 10% ethanolic potassium hydroxide. The compounds **6**–**9** and **14** were synthesized in a single step process by reaction of carbonyl chlorides with hydroxyl group of compounds **3**, **4**, and **5** in the presence of pyridine and 4-dimethylaminopyridine (4-DMAP) at 92–95 °C for 10–14 h. At the same time, compounds **10**–**13** and **15**–**16** were synthesized in two-step process. In the step-1, carboxyl group of compounds was converted into anhydride function by reacting with acetyl chloride in the presence of pyridine. In the step-II, anhydride function of respective compounds was reacted with hydroxyl group of compounds **3**, **4** and **5** in presence of 4-DMAP to yield compounds **10**–**13** and **15**–**16**. The 3-oxo group of compound **5** was reduced into hydroxyl group by using sodium borohydride to yield compound **17**. The 3β,22β-diacetoyloxy substituted compound **18** was synthesized from compound **17** by reaction of acetyl chloride with hydroxyl functions of **17** in the presence of 4-DMAP. Similarly, compound **19** was synthesized from compound **5** by means of esterification of carboxylic group using dimethyl sulfate. Whereas, the compound **19** was reduced by using sodium borohydride to yield compound **20**. The 3-hydroxylimino substituted compounds **21** and **22** were synthesized from **1** and **2**, by the reaction of hydroxylamine hydrochloride with 3-oxo group of **1** and **2**.

2.2. Biological screening

2.2.1. In vitro inhibition of TNF-α-induced NF-κB activation in A549 lung adenocarcinoma cell line

The human lung adenocarcinoma A549 cell line transiently co-transfected with NF-κB-luc was used to monitor the effects of lantadene congeners on tumor necrosis factor-alpha (TNF-α)-induced NF-κB activation. The compounds (**1**–**22**) were evaluated in a dose-dependent manner to determine the concentration needed to inhibit 50% of TNF-α-induced NF-κB activation (IC_{50}). The parent compounds **1**–**5** showed inhibition of TNF-α-induced NF-κB activation in the range of 6.42–0.98 μmol. The reduction of C-3 keto group of compounds **1** and **2** into C-3 hydroxyl group of compounds **4** and **5** led to increase in the activity, whereas hydrolysis of C-22 ester side chain of compound **1** and **2** into compound **5** led to decrease in the activity. The congeners of **3** and **4** showed inhibition of TNF-α-induced NF-κB activation in the range of >10–0.42 μmol, whereas the congeners of compound **5** showed $IC_{50} > 10$ μmol. It further confirmed that C-22 ester side chain played a critical role in the inhibition of TNF-α-induced NF-κB activation in A549 lung adenocarcinoma cell line. The hydrolysis of C-22 ester functionality in lantadenes led to significant reduction in activity, supporting the notion that the mechanism of inhibition is likely through a covalent Michael addition of nucleophiles (such as SH from cysteine) from protein candidate(s) to lantadenes (Fig. 1). The introduction of C-3 cinnamoyloxy functionality in parent compound **3** and **4** led to increase in the activity. This further confirmed the importance of strongly electrophilic α,β-unsaturated C=O group at C-22 and C-3 positions; played an important role in binding of compounds to the receptor site. The results of inhibition of TNF-α-induced NF-κB activation in A549 lung adenocarcinoma cell line by compounds **1**–**22** are shown in Table 1.

2.2.2. In vitro phosphorylation assay

The NF-κB can be activated by various signaling pathways and mostly through upstream kinase-based phosphorylation of IκBR. The phosphorylation of IκBR leads to degradation of proteasome and nucleus enrichment with p65 [14]. As compounds **12** and **13** showed potent NF-κB inhibition, therefore, we decided to evaluate the effect of parent compounds **3**, **4**, and its congeners **12**, and **13** against upstream kinase IKKβ that have been reported to activate the NF-κB pathway (Table 2). The compounds were evaluated *in vitro* for their inhibitory potency against the recombinant IKKβ in a non-radioisotope Kinase-Glo Luminescent Kinase Assays (Promega, U.S.A.). It was found that **12** and **13** remarkably inhibited IKKβ with IC_{50} of 1.20 and 0.94 μmol, respectively (Table 2).

2.2.3. Inhibitory activity against A549 lung cancer cells

Chronic inflammation of lungs results in lung carcinoma via activation of NF-κB [15]. Since, the lantadene congeners showed

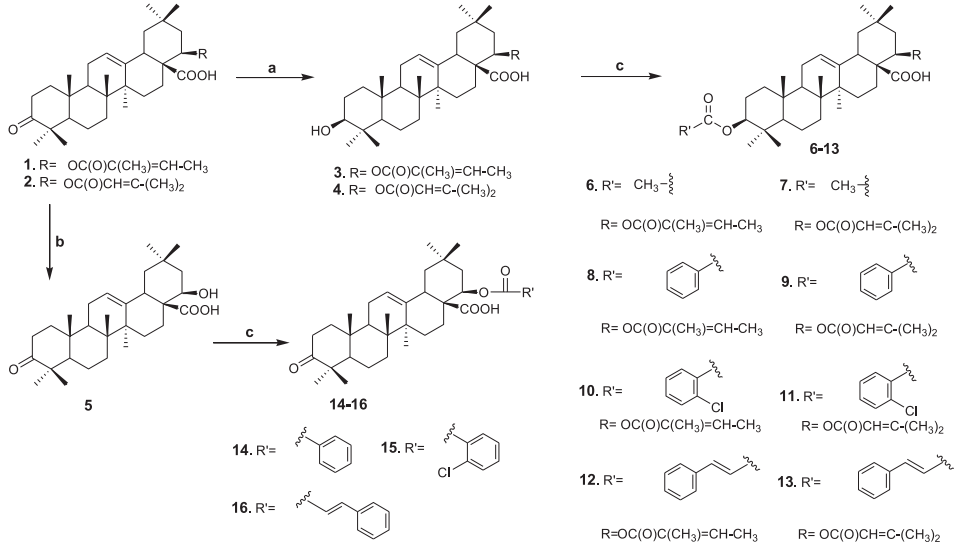

Scheme 1. Reagents and conditions: (a) $NaBH_4$, MeOH–THF, stir 7 h; (b) 10% ethanolic KOH, reflux 6 h; (c) R′–CO–Cl/R′COOCOCH$_3$, 4-DMAP, pyridine, reflux 92–95 °C, 10–14 h.

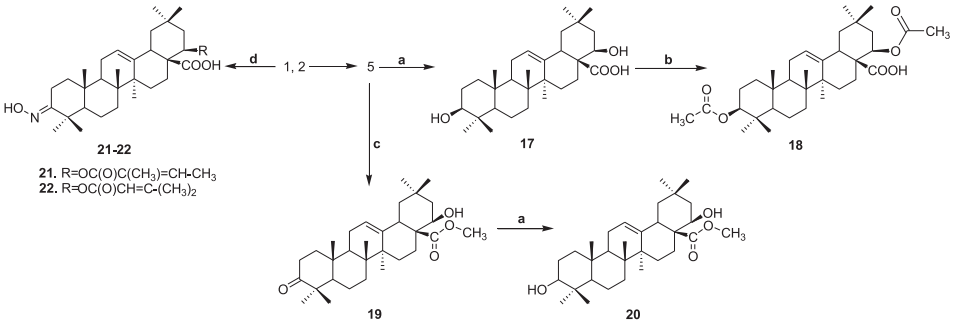

Scheme 2. Reagents and conditions: (a) $NaBH_4$, MeOH–THF, stir 7 h; (b) CH_3COCl, 4-DMAP, pyridine, reflux 92–95 °C, 10 h; (c) K_2CO_3, $(CH_3O)_2SO_2$, acetone, reflux, 12 h; (d) $NH_4OH.HCl$, pyridine, reflux 92–95 °C, 8 h.

marked inhibition of NF-κB, they were further evaluated for their *in vitro* cytotoxicity against lung cancer cells A549. The cytotoxicity profile of parent compounds (**1**–**5**) and ester congeners (**6**–**22**) are reported in Table 3. The parent pentacyclic triterpenoids **1**, **2**, **3**, and **4** showed cytotoxicity against A549 lung cancer cells with IC_{50} values of 2.84, 1.19, 0.79, and 0.43 μmol, respectively, whereas the compound **5** showed $IC_{50} > 10$ μmol. The C-3 cinnamoyloxy congener of compounds **3** and **4** showed marked cytotoxicity with IC_{50} of 0.12 and 0.08 μmol respectively (Table 3). From the cytotoxicity profiles of compounds **1**–**22**, it is evident that removal of the ester side chain at C-22 position led to decrease in the activity. The strongly electrophilic α,β-unsaturated carbonyl group of the ester side chain seems to play an important role in binding of compounds to the receptor site.

2.3. Predicting binding of lead ester congener *13* with IKKβ

Virtual screening of most potent ester congener **13** to IKKβ was carried out to rationalize the obtained biological results and to find out the possible binding mode of **13** with IKKβ. The lead ester congener **13** is a hybrid compound of two potent anticancer moieties i.e. reduced lantadene B and cinnamic acid, and at the site of action it is supposed to hydrolyzed back into parent moieties. Therefore, we docked both of the parent moieties, reduced lantadene B (moiety-A) and cinnamic acid (moiety-B) into the active site of IKKβ (PDB ID: 3QA8) [16] using AutoDock tools 1.5.4 (Fig. 2a–d).

The estimated free energy of binding of docked ester congener moiety-A was found to be −5.87 kcal/mol. Analyses of docked complex (Fig. 2a,b) indicated that 22β-senecioyloxy side chain and C-28 carboxylic group were critical for IKKβ inhibitory activity. Both the oxygens of ester function of 22β-senecioyloxy side chain interacted with amine hydrogens of Arg-31 by means of hydrogen bonding (O═C–O···H–N, 2.3 Å and O–C═O···H–N, 2.7 Å). Furthermore, carbonyl oxygen of ester group formed a hydrogen bond with Gln-40 residue of target protein (O–C═O···H–N, 2.2 Å). The hydroxyl oxygen of C-28 carboxylic group showed a hydrogen bond with hydroxyl hydrogen of Tyr-98 residue (O═C–O···H–O, 1.9 Å), whereas carbonyl oxygen of acid function exhibited hydrogen bonding with Gly-101 residue of IKKβ (O–C═O···H–N, 1.9 Å). Apart from hydrogen bonding, pentacyclic triterpenoid scaffold of the ester congener moiety-A also showed hydrophobic and van der Waal interactions with Leu-104, Val-152, Leu-153, Leu-160, and Ile-161 residues of the target protein, while 22β-senecioyloxy side chain demonstrated hydrophobic and van der Waal interactions with Leu-21 and Val-41 residues of IKKβ (Fig. 2b).

Estimated free energy of binding of ester congener moiety-B to IKKβ was found to be −4.65 kcal/mol. Analyses of docked complex (Fig. 2c,d) showed that hydroxyl oxygen of carboxylic function was hydrogen bonded to Tyr-98 (O═C–O···H–O, 2.0 Å), whereas carbonyl oxygen of carboxylic function formed a hydrogen bond with Gly-102 residue of IKKβ (O–C═O···H–N, 2.1 Å). In addition, carbonyl oxygen of ester congener moiety-B exhibited hydrogen bonding with Asp-103 residue of the target protein with a distance of 2.2 Å (O–C═O···H–N). Furthermore, both the oxygens of carboxylic acid function also interacted with Lys-106 residue of the target protein (O═C–O···H–N, 2.3 Å and O–C═O···H–N, 1.9 Å). Aromatic scaffold of moiety-B exhibited hydrophobic and van der Waal interactions with Met-96 and Ile-161 residues of the IKKβ protein (Fig. 2d). Besides hydrogen, hydrophobic and van der Waal interactions, the SH group of Cys-99 residue of IKKβ that acts as nucleophile was projected towards β-carbon of the 22β-senecioyloxy side chain of moiety-A. This indicates possible covalent Michael addition reaction between Cys-99 and β-carbon that might have played a central role in the IKKβ inhibitory potency of lead compound **13** (Figs. 1 and 2b).

2.4. Stability studies of ester congeners (*12* and *13*)

2.4.1. Chemical hydrolysis of lead ester congeners in simulated gastric fluid

A successful ester congener should be stable in the acidic pH of stomach. The compounds **12** and **13** that emerged as lead ester congeners from the synthesized series were further screened for their chemical stability studies. Ester congeners **12** and **13** were exposed to simulated gastric fluid of pH 2 for 0, 2, 5, 8, and 12 h. Results of HPLC analysis of ester congeners exposed to the simulated gastric fluid of pH 2 showed that only 0.0, 3.57, 9.33, 15.26, and 23.42% of **12** and 0.0, 2.80, 7.52, 12.39, and 18.95% of **13** were

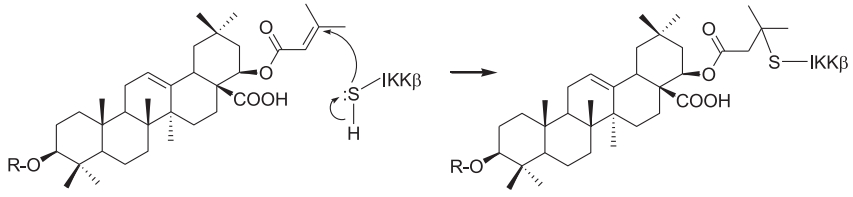

Fig. 1. Proposed covalent binding of IKKβ with ester congeners of lantadene, which leads to inhibition of NF-κB.

Table 1
TNF-α-induced NF-κB activation inhibitory activities (IC_{50} in μmol) of parent compounds (**1**–**5**), congeners (**6**–**22**).

Compd.	IC_{50}	Compd.	IC_{50}
1	1.06 ± 0.46	**14**	>10
2	1.56 ± 0.04	**15**	>10
3	0.98 ± 0.02	**16**	2.42 ± 0.24
4	1.02 ± 0.62	**17**	>10
5	6.42 ± 1.24	**18**	>10
6	2.80 ± 0.24	**19**	>10
7	2.32 ± 0.01	**20**	>10
8	5.04 ± 1.02	**21**	>10
9	4.64 ± 1.76	**22**	>10
10	4.18 ± 1.68		
11	3.70 ± 0.32		
12	0.56 ± 0.06		
13	0.42 ± 0.01		

Results are given as the mean of at least three independent experiments with triplicates in each experiment.

hydrolyzed after the exposure time of 0, 2, 5, 8, and 12 h, respectively (Table 4). The chemical structures of ester congeners **12** and **13** differ only at the ester side chain present in C-22 position. The 22β-angeloyloxy side chain is present in ester congener **12**, while 22β-senecioyloxy side chain is present in the ester congener **13**. It can be inferred from the results of chemical hydrolysis study that ester congener **13** showed slightly higher resistances towards hydrolysis in comparison to the **12** and both of them survived the stomach pH conditions.

2.4.2. *Metabolic stability of lead ester congeners (**12** and **13**) in human plasma*

To study plasma hydrolysis or susceptibility of ester congeners **12** and **13** towards human plasma esterases, they were exposed to 80% human plasma for 0, 15, 30, 60, and 120 min and extent of hydrolysis was monitored by HPLC. On exposure to human plasma, ester congeners **12** and **13** were hydrolyzed at a notably higher rate than the rate of their hydrolysis observed in the simulated gastric fluid. A level of ester congeners hydrolyzed was found to be 0.0, 25.84, 45.32, and 53.19, and 63.25% of **12** and 0.0, 25.78, 44.50, 51.87, and 60.76% of **13** after the exposure period of 0, 15, 30, 60, and 120 min, respectively (Table 5). Ester congener **13** showed slightly lesser degree of hydrolysis than ester congener **12**. HPLC results indicated that ester congeners **12** and **13** underwent rapid hydrolysis in human plasma to liberate the parent drug molecules to reach the site of action, while in the simulated gastric fluid of pH 2, they survived the stomach conditions. Stability of an ester bond depends on the reactivity of carbonyl carbon, as it gets attacked by the reactive functional groups. The oxygen atom (oxygen atom neighboring to carbonyl carbon of ester bond) of ester function of synthesized ester congeners is an electron withdrawing in nature, and therefore, it decreases the electron density on the carbonyl carbon. In this course, electron deficient carbonyl carbon will become more prone to experience a nucleophilic attack and eventually undergoes hydrolysis. The ester congener **13** showed slower rate of hydrolysis than **12**, because it possessed geminal methyl groups in the proximity of ester function. The geminal methyl groups will have slightly higher ability to decrease the electrophilicity of ester carbonyl carbon. On the contrary, methyl groups of the side chain of ester congener **12** were present in the vicinal position and therefore, **12** exhibited slightly higher degree of hydrolysis than **13**.

Table 2
In vitro IKKβ inhibition by parent compounds (**3** and **4**) and congener (**12** and **13**).

Compd.	IC_{50} (μmol)
3	2.62 ± 0.82
4	4.24 ± 0.94
12	1.20 ± 0.42
13	0.94 ± 0.04

Results are given as the mean of at least three independent experiments with triplicates in each experiment.

3. Conclusion

The C-3, C-22 and C-17 congeners of pentacyclic triterpenoids **3** and **4** showed marked cytotoxicity and inhibitory potential against TNF-α-induced activation of NF-κB in lung cancer cell line A549. The congeners of **5** showed feeble activity, supporting the perception that the mechanism of inhibition is likely through a covalent Michael addition of nucleophiles (such as SH from cysteine) from protein candidate(s) to reduced lantadenes. The ester congener **13** inhibited kinase activity of IKKβ in a single-digit micromolar concentration. The experimental and docking studies revealed that C-22 ester side chain with α,β-unsaturated carbonyl group was critical for the activity. Moreover, ester congener **13** showed stability in the acidic pH and was hydrolyzed readily in the human blood plasma to release the two active moieties. The lead congener **12** and **13** are promising anticancer candidates against lung cancer, warranting further investigations.

4. Experimental

4.1. Material and methods

Merck TLC plates silica gel 60 F_{254} (Merck, Germany) were used to monitor the progress of reactions. Melting points reported are uncorrected and were recorded on a digital melting point apparatus (Indosati scientific lab equipments, India). Chromatography columns of appropriate sizes were used with silica gel (100–200 mesh) as adsorbent. FT-IR spectra were recorded on a PerkinElmer spectrum 400 FT-IR and FT-NIR spectrometer using potassium bromide pellets. ^1H NMR and ^{13}C NMR spectra were recorded at 400 and 100 MHz, respectively with Bruker AVANCE II 400 NMR spectrometer using $CDCl_3$, DMSO-d_6, and a mixture of $CDCl_3$ and DMSO-d_6 as solvents, and tetramethylsilane was used as internal standard. ESI-MS spectra were recorded with Waters Micromass Q-T of micro Mass spectrometer using electrospray ionization at 70 eV. For elemental analysis of compounds, 2400 CHN analyzer (PerkinElmer, USA) was used. All the reagents and anhydrous

Table 3
In vitro cytotoxicity profile (IC_{50} in μmol) of parent compounds (**1**–**5**) and congeners (**6**–**22**) against A549 cell line.

Compd.	IC_{50}	Compd.	IC_{50}
1	2.84 ± 0.72	**14**	>10
2	1.19 ± 0.28	**15**	>10
3	0.79 ± 0.01	**16**	3.64 ± 1.24
4	0.43 ± 0.03	**17**	>10
5	>10	**18**	>10
6	5.42 ± 1.24	**19**	>10
7	4.90 ± 1.20	**20**	>10
8	7.36 ± 1.06	**21**	>10
9	7.20 ± 1.20	**22**	>10
10	6.80 ± 2.40	Cisplatin	21.3 ± 3.62
11	6.52 ± 2.32		
12	0.12 ± 0.02		
13	0.08 ± 0.02		

Results are given as the mean of at least three independent experiments with triplicates in each experiment.

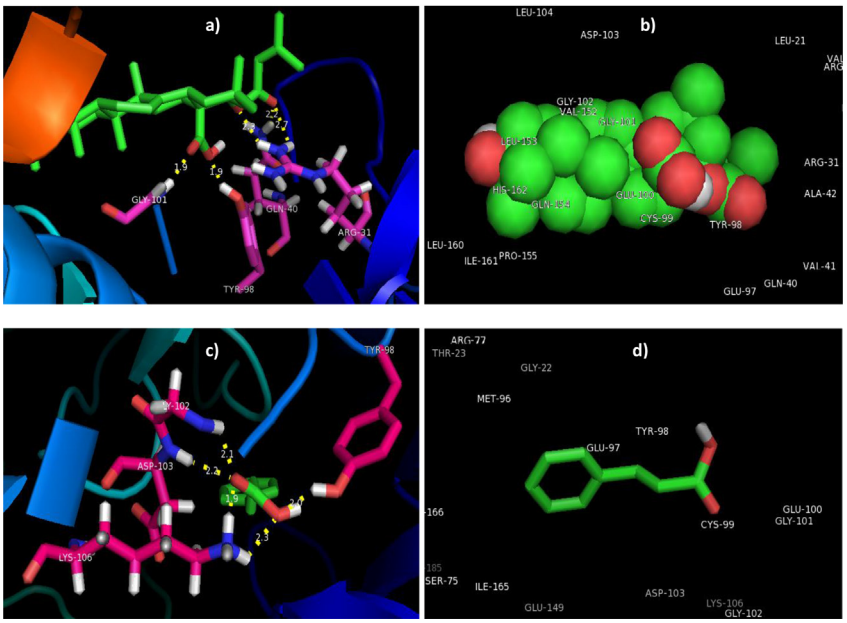

Fig. 2. (a) Binding of ester congener moiety-A of **13** into the binding site of IKKβ. The amino acids Arg-31, Gln-40, Tyr-98, and Gly-101 involved in the hydrogen bond interactions with ester congener moiety-A, are highlighted; (b) stereoview of the docked structure of ester congener moiety-A of **13** into the active site of IKKβ. The amino acid residues involved in hydrogen, hydrophobic, and van der Waal interactions with ester congener moiety-A, are highlighted; (c) binding of ester congener moiety-B of **13** within the active site of IKKβ. The amino acid residues Tyr-98, Gly-102, Asp-103, and Lys-106 involved in the hydrogen bond interactions with ester congener moiety-B, are highlighted; (d) docking of ester congener moiety-B of **13** into the active site of IKKβ. The amino acid residues engaged in hydrogen, hydrophobic, and van der Waal interactions with ester congener moiety-B, are highlighted.

solvents were purchased from local Indian suppliers and were used without further purification or distillation, unless otherwise stated. For RP-HPLC analysis, Waters HPLC system comprised of Waters 717plus autosampler, Waters 515 HPLC pumps, Waters Spherisorb ODS2 (80 Å, 5 μm, 4.6 × 250 mm) C18 column, Waters 2996 PDA detector, and empower software system 2.1 was used.

4.2. Plant material

Leaves of *L. camara* L. were collected in September 2010 from Palampur (HP), India. The leaves were shade-dried and powdered. A voucher specimen (LC; 097 JUIT) was deposited in the Herbarium at the Jaypee University of Information Technology Waknaghat, India.

4.3. Extraction and isolation of lantadene A (*1*) and B (*2*)

Extraction and isolation of lantadene A (**1**) and B (**2**) were carried out as per our previously reported procedure with slight modifications (Supplementary data: page 6–7) [17].

4.4. Synthesis of 3β-hydroxy-22β-angeloyloxy-olean-12-en-28-oic acid (*3*) and 3β-hydroxy-22β-senecioyloxy-olean-12-en-28-oic acid (*4*)

Reduced lantadene A (**3**) and B (**4**) were synthesized as per procedure reported by us previously (Scheme 1) (Supplementary data: page 7–8) [17].

4.5. Synthesis of 22β-hydroxy-3-oxo-olean-12-en-28-oic acid (*5*)

Compound **5** was synthesized from compound **1** and **2** as per procedure described by us previously with slight modifications (Scheme 1) (Supplementary data: page 8–9) [12].

4.6. Synthesis of 3β-substituted and 22β-substituted olean-12-en-28-oic acids (*6*–*16*)

Compounds **6**–**9**, **14** were synthesized through a single step process, while compounds **10**–**13** and **15**–**16** were synthesized via two step processes. In the first step of synthesis of compounds **10**–**13** and **15**–**16**, acid function was converted into anhydride function (Supplementary data: Scheme S1). The acid and acetyl chloride in the presence of pyridine were refluxed in dichloromethane (DCM) for 4–5 h. Reaction mixture was concentrated and washed with chloroform (100 ml × 3) under reduced pressure at 60–65 °C to afford solid to semisolid anhydride products of respective acids, which were used in the next step without further purification.

In the synthesis of 3β-substituted (**6**–**13**) and 22β-substituted (**14**–**16**) olean-12-en-28-oic acids step, compounds **3**, **4**, and **5** with appropriate carbonyl chlorides/anhydrides were refluxed in pyridine in the presence of 4-DMAP for 10–14 h at 92–95 °C (Scheme 1). Reaction mixture was poured into 10% HCl solution and precipitated product was extracted with DCM and washed further three times with 10% HCl solution (100 ml × 3). Organic layer was evaporated to dryness and the reaction mixture obtained was chromatographed over silica gel (100–200 mesh) and eluted with varying ratio of hexane–ethyl acetate to give purified products (**6**–**16**).

4.6.1. 3β-Acetoyloxy-22β-angeloyloxy-olean-12-en-28-oic acid (*6*)

Yield: 84.10%, mp: 178–180 °C. Anal. calcd. for $C_{37}H_{56}O_6$ (596.41): %C, 74.46; H, 9.46. Found: %C, 74.50; H, 9.45. IR (KBr, cm^{-1}): 2950.19, 2877.28 (C–H), 1736.33 (C=O ester), 1719.91 (C=O acid), 1649.60 (C=C). ^{1}H NMR (400 MHz, $CDCl_3$, δ ppm): 5.8822–5.9399 (1H, m, C-33-H), 5.2740–5.2889 (1H, t, J = 2.98 Hz, C-12-H), 4.9972–5.0118 (1H, t, J = 2.92 Hz, C-22-H), 4.4116–4.4512 (1H, t, J = 7.92 Hz, C-3-H), 2.9424–2.9862 (1H, dd, J = 13.92, 3.96 Hz, C-18-H), 1.9830 (3H, s, C-2′-H), 1.0885 (3H, s, CH_3), 0.9247 (3H, s, CH_3), 0.8730 (3H, s, CH_3), 0.8227 (3H, s, CH_3), 0.8015 (3H, s, CH_3), 0.7957

Table 4
Chemical stability of ester congeners (**12**–**13**) in simulated gastric fluid of pH 2.

Time	% Ester congener remaining in simulated gastric fluid	
	Compd. **12**	Compd. **13**
0 h	100	100
2 h	96.43	97.20
5 h	90.67	92.48
8 h	84.74	87.61
12 h	76.58	81.05

(3H, s, CH_3), 0.6959 (3H, s, CH_3). ^{13}C NMR (100 MHz, $CDCl_3$, δ ppm): 179.56 (C-28), 171.12 (C-1′), 166.34 (C-31), 143.08 (C-13), 138.79 (C-33), 127.69 (C-32), 122.62 (C-12), 80.88 (C-3), 75.96 (C-22), 55.26 (C-5), 50.54 (C-17), 47.55 (C-9), 45.97 (C-19), 41.83 (C-14) 39.22 (C-8), 38.35 (C-18), 38.28 (C-4), 38.07 (C-1), 37.70 (C-21), 36.95 (C-10), 33.70 (C-29), 32.55 (C-7), 30.04 (C-20), 28.04 (C-15), 27.55(C-23), 26.15 (C-27), 25.85 (C-30), 24.20 (C-16), 23.51 (C-11), 23.43 (C-2), 21.35 (C-2′), 20.56 (C-6), 18.11 (C-35), 17.01 (C-26), 16.70 (C-24), 15.65 (C-34), 15.51 (C-25). ESI-MS (negative-ion mode, *m*/*z*): 596.30 (M^-), 595.30 ($M^- - 1$).

*4.6.2. 3β-Acetoyloxy-22β-senecioyloxy-olean-12-en-28-oic acid (**7**)*

Yield: 82.09%, mp: 172–174 °C. Anal. calcd. for $C_{37}H_{56}O_6$ (596.41): %C, 74.46; H, 9.46. Found: %C, 74.49; H, 9.47. IR (KBr, cm^{-1}): 2949.03 (C–H), 1720.98 (C=O acid), 1653.63 (C=C). ^1H NMR (400 MHz, $CDCl_3$, δ ppm): 5.4733–5.4789 (1H, t, J = 1.12 Hz, C-32-H), 5.2685–5.2841 (1H, t, J = 3.12 Hz, C-12-H), 4.9927–5.0069 (1H, t, J = 2.84 Hz, C-22-H), 4.4113–4.4508 (1H, t, J = 7.90 Hz, C-3-H), 2.9395–2.9834 (1H, dd, J = 13.92, 3.92 Hz, C-3-H), 1.9825 (3H, s, C-2′-H), 1.0870 (3H, s, CH_3), 0.9227 (3H, s, CH_3), 0.8722 (3H, s, CH_3), 0.8213 (3H, s, CH_3), 0.8007 (3H, s, CH_3), 0.7959 (3H, s, CH_3), 0.6922 (3H, s, CH_3). ^{13}C NMR (100 MHz, $CDCl_3$, δ ppm): 180.09 (C-28), 171.14 (C-1′), 166.33 (C-31), 157.16 (C-33), 143.09 (C-13), 122.59 (C-12), 115.95 (C-32), 80.88 (C-3), 75.96 (C-22), 55.25 (C-5), 50.55 (C-17), 47.55 (C-9), 45.97 (C-19), 41.81 (C-14) 39.21 (C-8), 38.29 (C-18), 38.24 (C-4), 38.06 (C-1), 37.69 (C-21), 36.95 (C-10), 33.70 (C-29), 32.53 (C-7), 30.04 (C-20), 28.04 (C-15), 27.53 (C-23), 27.49 (C-35), 26.15 (C-27), 25.85 (C-30), 24.20 (C-16), 23.50 (C-11), 23.43 (C-2), 21.34 (C-2′), 20.56 (C-6), 18.39 (C-34), 17.02 (C-26), 16.69 (C-24), 15.50 (C-25). ESI-MS (negative-ion mode, *m*/*z*): 596.30 (M^-), 595.30 ($M^- - 1$).

*4.6.3. 3β-Benzoyloxy-22β-angeloyloxy-olean-12-en-28-oic acid (**8**)*

Yield: 90.00%, mp: 117–119 °C. Anal. calcd. for $C_{42}H_{58}O_6$ (658.42): %C, 76.56; H, 8.87. Found: %C, 76.55; H, 8.88. IR (KBr, cm^{-1}): 3064.72, 2950.36, 2876.88 (C–H), 1716.97 (C=O), 1650.27 (C=C). ^1H NMR (400 MHz, $CDCl_3$, δ ppm): 8.0325–8.0887 (2H, m, C-3′ & C-7′-Ar-H), 7.5310–7.6216 (1H, m, C-5′-Ar-H), 7.4215–7.4646 (2H, m, C-4′ & C-6′-Ar-H), 5.9550–6.0677 (1H, m, C-33-H), 5.3776–5.3950 (1H, t, J = 3.48 Hz, C-12-H), 5.0955–5.1105 (1H, t, J = 3.00 Hz, C-22-H), 4.7317–4.7724 (1H, m, C-3-H), 3.0441–3.0865 (1H, dd, J = 13.64, 4.40 Hz, C-18-H), 1.1947 (3H, s, CH_3), 1.0267 (3H, s, CH_3), 1.0142 (3H, s, CH_3), 1.0058 (3H, s, CH_3), 0.9493 (3H, s, CH_3), 0.9077 (3H, s, CH_3), 0.8131 (3H, s, CH_3). ^{13}C NMR (100 MHz, $CDCl_3$, δ ppm): 181.10 (C-28), 166.52 (C-31), 166.31 (C-1′), 142.30 (C-13), 139.84 (C-33), 132.74 (C-5′), 130.44 (C-2′), 129.54 (C-3′ & C-7′), 128.71 (C-32), 128.33 (C-4′ & C-6′), 123.35 (C-12), 81.58 (C-3), 75.97 (C-22), 55.45 (C-5), 50.61 (C-17), 47.66 (C-9), 45.90 (C-19), 42.13 (C-14), 39.53 (C-8), 39.30 (C-18), 38.77 (C-4), 38.12 (C-1), 37.99 (C-21), 37.01 (C-10), 33.71 (C-29), 32.62 (C-7), 30.06 (C-20), 28.21 (C-15), 27.63 (C-23), 26.18 (C-27), 25.88 (C-30), 25.75 (C-16), 23.59 (C-11), 23.47 (C-2), 20.45 (C-6), 18.21 (C-35), 16.98 (C-26), 16.73 (C-24), 15.63 (C-34), 15.52 (C-25). ESI-MS (negative-ion mode, *m*/*z*): 658.00 (M^-), 657.20 ($M^- - 1$).

Table 5
Metabolic stability of ester congeners (**12**–**13**) in human plasma.

Time	% Ester congener remaining in human plasma	
	Compd. **12**	Compd. **13**
0 min	100	100
15 min	74.16	74.72
30 min	54.68	55.50
60 min	46.81	48.13
120 min	36.75	39.24

*4.6.4. 3β-Benzoyloxy-22β-senecioyloxy-olean-12-en-28-oic acid (**9**)*

Yield: 88.17%, mp: 115–116 °C. Anal. calcd. for $C_{42}H_{58}O_6$ (658.42): %C, 76.56; H, 8.87. Found: %C, 76.60; H, 8.85. IR (KBr, cm^{-1}): 2950.46, 2877.90, 2665.64 (C–H), 1716.35 (C=O), 1649.60 (C=C). ^1H NMR (400 MHz, $CDCl_3$, δ ppm): 8.0327–8.0921 (2H, m, C-3′ & C-7′-Ar-H), 7.5285–7.6294 (1H, m, C-5′-Ar-H), 7.4187–7.4861 (2H, m, C-4′ & C-6′-Ar-H), 5.5628–5.5689 (1H, t, J = 1.22 Hz, C-32-H), 5.3730–5.3896 (1H, t, J = 3.32 Hz, C-12-H), 5.0464–5.0615 (1H, t, J = 3.02 Hz, C-22-H), 4.7309–4.7716 (1H, m, C-3-H), 3.0210–3.0653 (1H, dd, J = 13.72, 4.04 Hz, C-18-H), 1.1943 (3H, s, CH_3), 1.0264 (3H, s, CH_3), 1.0167 (3H, s, CH_3), 1.0062 (3H, s, CH_3), 0.9499 (3H, s, CH_3), 0.8970 (3H, s, CH_3), 0.8201 (3H, s, CH_3). ^{13}C NMR (100 MHz, $CDCl_3$, δ ppm): 179.16 (C-28), 166.31 (C-31), 165.34 (C-1′), 157.12 (C-33), 143.06 (C-13), 132.74 (C-5′), 130.95 (C-2′), 129.54 (C-3′ & C-7′), 128.33 (C-4′ & C-6′), 122.57 (C-12), 115.99 (C-32), 81.52 (C-3), 75.28 (C-22), 55.38 (C-5), 50.63 (C-17), 47.59 (C-9), 46.01 (C-19), 41.96 (C-14), 39.31 (C-8), 38.47 (C-18), 38.19 (C-4), 38.11 (C-1), 37.68 (C-21), 37.01 (C-10), 33.79 (C-29), 32.64 (C-7), 30.09 (C-20), 28.22 (C-15), 27.63 (C-23), 27.42 (C-35), 26.31 (C-27), 25.88 (C-30), 24.14 (C-16), 23.59 (C-11), 23.51 (C-2), 20.22 (C-6), 18.20 (C-34), 16.98 (C-26), 16.96 (C-24), 15.54 (C-25). ESI-MS (negative-ion mode, *m*/*z*): 658.30 (M^-), 657.00 ($M^- - 1$).

*4.6.5. 3β-(2-Chlorobenzoyloxy)-22β-angeloyloxy-olean-12-en-28-oic acid (**10**)*

Yield: 85.53%, mp: 176–178 °C. Anal. calcd. for $C_{42}H_{57}ClO_6$ (692.38): %C, 72.76; H, 8.29. Found: %C, 72.82; H, 8.31. IR (KBr, cm^{-1}): 2948.62, 2877.90 (C–H), 1720.58 (C=O), 1548.70 (C=C). ^1H NMR (400 MHz, $CDCl_3$, δ ppm): 7.7959–7.8191 (1H, m, C-7′-Ar-H), 7.3828–7.4741 (2H, m, C-4′ & C-5′-Ar-H), 7.2916–7.3325 (1H, m, C-6′-Ar-H), 5.9508–6.0081 (1H, m, C-33-H), 5.3552–5.3709 (1H, t, J = 3.14 Hz, C-12-H), 5.0753–5.0892 (1H, t, J = 2.78 Hz, C-22-H), 4.7682–4.8085 (1H, m, C-3-H), 3.0253–3.0687 (1H, dd, J = 13.68, 3.72 Hz, C-18-H), 1.1884 (3H, s, CH_3), 0.9928 (3H, s, CH_3), 0.9828 (3H, s, CH_3), 0.9761 (3H, s, CH_3), 0.9450 (3H, s, CH_3), 0.9006 (3H, s, CH_3), 0.7889 (3H, s, CH_3). ^{13}C NMR (100 MHz, $CDCl_3$, δ ppm): 181.40 (C-28), 166.35 (C-1′), 165.71 (C-31), 143.11 (C-13), 138.78 (C-33), 133.48 (C-5′), 132.30 (C-3′), 131.26 (C-7′), 131.05 (C-4′), 130.93 (C-2′), 127.67 (C-32), 126.56 (C-6′), 122.59 (C-12), 82.63 (C-3), 75.99 (C-22), 55.38 (C-5), 50.59 (C-17), 47.57 (C-9), 45.98 (C-19), 41.87 (C-14), 39.22 (C-8), 38.25 (C-18), 38.17 (C-4), 37.96 (C-1), 37.69 (C-21), 36.99 (C-10), 33.70 (C-29), 32.55 (C-7), 30.07 (C-20), 28.21 (C-15), 27.55 (C-23), 26.15 (C-27), 25.91 (C-30), 24.22 (C-16), 23.50 (C-11), 23.46 (C-2), 20.56 (C-6), 18.13 (C-35), 17.02 (C-26), 16.70 (C-24), 15.65 (C-34), 15.53 (C-25). ESI-MS (negative-ion mode, *m*/*z*): 691.60 (M^-).

*4.6.6. 3β-(2-Chlorobenzoyloxy)-22β-senecioyloxy-olean-12-en-28-oic acid (**11**)*

Yield: 84.52%, mp: 170–172 °C. Anal. calcd. for $C_{42}H_{57}ClO_6$ (692.38): %C, 72.76; H, 8.29. Found: %C, 72.79; H, 8.30. IR (KBr,

cm^{-1}): 2949, 2877 (C–H), 1717 (C=O), 1651 (C=C). ^1H NMR (400 MHz, $CDCl_3$, δ ppm): 7.7950–7.8183 (1H, m, C-7′-Ar-H), 7.3818–7.4814 (2H, m, C-4′ & C-5′-Ar-H), 7.2909–7.3319 (1H, m, C-6′-Ar-H), 5.5659–5.5721 (1H, t, $J = 1.24$ Hz, C-32-H), 5.3732–5.3897 (1H, t, $J = 3.30$ Hz, C-12-H), 5.0436–5.0578 (1H, t, $J = 2.84$ Hz, C-22-H), 4.7666–4.8069 (1H, m, C-3-H), 3.0136–3.0580 (1H, dd, $J = 13.56$, 4.44 Hz, C-18-H), 1.1922 (3H, s, CH_3), 1.0137 (3H, s, CH_3), 0.9908 (6H, s, 2× CH_3), 0.9799 (3H, s, CH_3), 0.8939 (3H, s, CH_3), 0.8124 (3H, s, CH_3). ^{13}C NMR (100 MHz, $CDCl_3$, δ ppm): 178.49 (C-28), 165.41 (C-1′), 164.66 (C-31), 156.13 (C-33), 142.02 (C-13), 132.46 (C-5′), 131.34 (C-3′), 130.21 (C-7′), 130.01 (C-4′), 129.94 (C-2′), 125.52 (C-6′), 121.49 (C-12), 114.92 (C-32), 81.61 (C-3), 74.22 (C-22), 54.37 (C-5), 49.57 (C-17), 46.54 (C-9), 44.95 (C-19), 40.89 (C-14), 38.25 (C-8), 37.37 (C-18), 37.17 (C-4), 36.93 (C-1), 36.66 (C-21), 35.96 (C-10), 32.72 (C-29), 31.56 (C-7), 29.04 (C-20), 27.17 (C-15), 26.56 (C-23), 26.42 (C-35), 25.27 (C-27), 25.11 (C-30), 24.85 (C-16), 23.17 (C-11), 23.11 (C-2), 19.20 (C-6), 17.13 (C-34), 15.98 (C-26), 15.94 (C-24), 14.49 (C-25). ESI-MS (negative-ion mode, m/z): 691.60 (M^-).

4.6.7. 3β-Cinnamoyloxy-22β-angeloyloxy-olean-12-en-28-oic acid (**12**)

Yield: 89.50%, mp: 174–176 °C. Anal. calcd. for $C_{44}H_{60}O_6$ (684.44): %C, 77.16; H, 8.83. Found: %C, 77.13; H, 8.85. IR (KBr, cm^{-1}): 3266 (O–H of COOH), 2950, 2877 (C–H), 1719 (C=O), 1649 (C=C). ^1H NMR (400 MHz, $CDCl_3$, δ ppm): 7.6478–7.6878 (1H, d, $J = 16$ Hz, C-3′-H), 7.5207–7.5446 (2H, m, C-5′ & C-9′-Ar-H), 7.3725–7.3890 (3H, m, C-6′, C-8′ & C-7′-Ar-H), 6.4243–6.4643 (1H, d, $J = 16$ Hz, C-2′-H), 5.9749–6.0328 (1H, m, C-33-H), 5.3658–5.3833 (1H, t, $J = 3.50$ Hz, C-12-H), 5.0882–5.1019 (1H, t, $J = 2.74$ Hz, C-22-H), 4.6313–4.6713 (1H, t, $J = 8.00$ Hz, C-3-H), 3.0294–3.0740 (1H, dd, $J = 13.96$, 3.92 Hz, C-18-H), 1.1817 (3H, s, CH_3), 1.0093 (3H, s, CH_3), 0.9796 (3H, s, CH_3), 0.9532 (3H, s, CH_3), 0.9234 (3H, s, CH_3), 0.9029 (3H, s, CH_3), 0.7933 (3H, s, CH_3). ^{13}C NMR (100 MHz, $CDCl_3$, δ ppm): 179.30 (C-28), 165.85 (C-31), 165.28 (C-1′), 143.35 (C-3′), 142.06 (C-13), 137.75 (C-33), 133.47 (C-4′), 129.15 (C-7′), 127.83 (C-6′ & C-8′), 127.02 (C-5′ & C-9′), 126.63 (C-32), 121.57 (C-12), 116.30 (C-2′), 79.89 (C-3), 74.94 (C-22), 54.27 (C-5), 49.54 (C-17), 46.53 (C-9), 44.95 (C-19), 40.80 (C-14), 38.21 (C-8), 37.20 (C-18), 37.07 (C-4), 36.92 (C-1), 36.66 (C-21), 35.95 (C-10), 32.66 (C-29), 31.51 (C-7), 29.01 (C-20), 27.08 (C-15), 26.51 (C-23), 25.11 (C-27), 24.85 (C-30), 23.19 (C-16), 22.58 (C-11), 22.41 (C-2), 19.52 (C-6), 17.09 (C-35), 16.02 (C-26), 15.84 (C-24), 14.61 (C-34), 14.47 (C-25). ESI-MS (negative-ion mode, m/z): 683.70 (M^-).

4.6.8. 3β-Cinnamoyloxy-22β-senecioyloxy-olean-12-en-28-oic acid (**13**)

Yield: 85.99%, mp: 165–166 °C. Anal. calcd. for $C_{44}H_{60}O_6$ (684.44): %C, 77.16; H, 8.83. Found: %C, 77.23; H, 8.84. IR (KBr, cm^{-1}): 3240 (O–H of COOH), 2947, 2875 (C–H), 1745 (C=O ester), 1715 (C=O acid), 1635 (C=C). ^1H NMR (400 MHz, $CDCl_3$, δ ppm): 7.6488–7.6887 (1H, d, $J = 15.96$ Hz, C-3′-H), 7.5206–7.5445 (2H, m, C-5′ & C-9′-Ar-H), 7.3722–7.3885 (3H, m, C-6′, C-8′ & C-7′-Ar-H), 6.4254–6.4654 (1H, d, $J = 16$ Hz, C-2′-H), 5.5490–5.5552 (1H, t, $J = 1.24$ Hz, C-32-H), 5.3506–5.3683 (1H, t, $J = 3.54$ Hz, C-12-H), 5.0753–5.0874 (1H, t, $J = 2.37$ Hz, C-22-H), 4.6323–4.6722 (1H, t, $J = 7.98$ Hz, C-3-H), 3.0231–3.0646 (1H, dd, $J = 13.92$, 3.52 Hz, C-18-H), 1.1778 (3H, s, CH_3), 1.0006 (3H, s, CH_3), 0.9776 (3H, s, CH_3), 0.9539 (3H, s, CH_3), 0.9230 (3H, s, CH_3), 0.8987 (3H, s, CH_3), 0.7826 (3H, s, CH_3). ^{13}C NMR (100 MHz, $CDCl_3$, δ ppm): 180.12 (C-28), 166.83 (C-31), 166.27 (C-1′), 157.13 (C-33), 144.33 (C-3′), 143.04 (C-13), 134.45 (C-4′), 130.14 (C-7′), 128.82 (C-6′ & C-8′), 128.00 (C-5′ & C-9′), 122.57 (C-12), 118.71 (C-2′), 115.89 (C-32), 80.87 (C-3), 75.91 (C-22), 55.25 (C-5), 50.51 (C-17), 47.51 (C-9), 45.92 (C-19), 41.78 (C-14), 39.18 (C-8), 38.20 (C-18), 38.05 (C-4), 37.90 (C-1), 37.64 (C-21), 36.93 (C-10), 33.65 (C-29), 32.50 (C-7), 29.99 (C-20), 28.06 (C-15), 27.99 (C-23), 27.49 (C-35), 26.10 (C-27), 25.83 (C-30), 24.17 (C-16), 23.57 (C-11), 23.40 (C-2), 20.52 (C-6), 18.06 (C-34), 16.99 (C-26), 16.82 (C-24), 15.48 (C-25). ESI-MS (negative-ion mode, m/z): 683.70 (M^-).

4.6.9. 22β-Benzoyloxy-3-oxo-olean-12-en-28-oic acid (**14**)

Yield: 55.15%, mp: 123–124 °C. Anal. calcd. for $C_{37}H_{50}O_5$ (574.37): %C, 77.31; H, 8.77. Found: %C, 77.25; H, 8.75. IR (KBr, cm^{-1}): 2949.41 (C–H), 1720.54 (C=O), 1603.96 (C=C). ^1H NMR (400 MHz, $CDCl_3$, δ ppm): 7.7746–7.7974 (2H, m, C-3′ & C-7′-Ar-H), 7.3507–7.3908 (1H, m, C-5′-Ar-H), 7.2097–7.2294 (2H, m, C-4′ & C-6′-Ar-H), 5.3667–5.3839 (1H, t, $J = 3.44$ Hz, C-12-H), 5.1223–5.1373 (1H, t, $J = 3.00$ Hz, C-22-H), 3.0982–3.1430 (1H, dd, $J = 13.80$, 4.12 Hz, C-18-H), 2.4412–2.5270 (1H, m, C-2-Ha), 2.2664–2.3317 (1H, m, C-2-Hb), 1.1857 (3H, s, CH_3), 1.1249 (3H, s, CH_3), 1.0218 (3H, s, CH_3), 0.9854 (3H, s, CH_3), 0.8841 (3H, s, CH_3), 0.8210 (3H, s, CH_3), 0.7370 (3H, s, CH_3). ^{13}C NMR (100 MHz, $CDCl_3$, δ ppm): 217.68 (C-3), 178.11 (C-28), 165.12 (C-1′), 143.09 (C-13), 132.90 (C-5′), 130.06 (C-2′), 129.47 (C-3′ & C-7′), 128.28 (C-4′ & C-6′), 122.63 (C-12), 76.82 (C-22), 55.32 (C-5), 50.69 (C-17), 47.44 (C-9), 46.87 (C-4), 45.96 (C-19), 42.09 (C-14), 39.23 (C-8), 39.11 (C-18), 38.52 (C-1), 37.60 (C-21), 36.78 (C-10), 34.12 (C-2), 33.66 (C-29), 32.19 (C-7), 29.98 (C-20), 27.61 (C-15), 26.46 (C-23), 26.26 (C-27), 25.80 (C-30), 24.01 (C-16), 23.53 (C-11), 21.49 (C-6), 19.54 (C-26), 16.81 (C-24), 15.11 (C-25). ESI-MS (negative-ion mode, m/z): 574.30 (M^-), 573.30 ($M^- - 1$).

4.6.10. 22β-(2-Chlorobenzoyloxy)-3-oxo-olean-12-en-28-oic acid (**15**)

Yield: 49.57%, mp: 193–195 °C. Anal. calcd. for $C_{37}H_{49}ClO_5$ (608.33): %C, 72.94; H, 8.11. Found: %C, 72.93; H, 8.13. IR (KBr, cm^{-1}): 2955.55, 2927.40, 2874.30 (C–H), 1735.52 (C=O keto), 1703.58 (C=O), 1591.67 (C=C). ^1H NMR (400 MHz, $CDCl_3$, δ ppm): 7.8866–7.9101 (1H, m, C-7′-Ar-H), 7.3686–7.4244 (2H, m, C-4′ & C-5′-Ar-H), 7.2473–7.2884 (1H, m, C-6′-Ar-H), 5.3250–5.3424 (1H, t, $J = 3.48$ Hz, C-12-H), 5.2060–5.2206 (1H, t, $J = 2.92$ Hz, C-22-H), 3.0374–3.0820 (1H, dd, $J = 13.76$, 4.24 Hz, C-18-H), 2.4468–2.5326 (1H, m, C-2-Ha), 2.2759–2.3412 (1H, m, C-2-Hb), 1.1811 (3H, s, CH_3), 1.1258 (3H, s, CH_3), 1.0210 (3H, s, CH_3), 0.9776 (3H, s, CH_3), 0.8789 (3H, s, CH_3), 0.8395 (3H, s, CH_3), 0.7925 (3H, s, CH_3). ^{13}C NMR (100 MHz, $CDCl_3$, δ ppm): 217.99 (C-3), 180.46 (C-28), 170.27 (C-1′), 142.91 (C-13), 133.34 (C-5′), 132.37 (C-3′), 131.41 (C-7′), 130.96 (C-4′), 129.28 (C-2′), 126.62 (C-6′), 122.61 (C-12), 77.37 (C-22), 55.22 (C-5), 50.67 (C-17), 47.41 (C-9), 46.83 (C-4), 45.80 (C-19), 41.95 (C-14), 39.21 (C-8), 39.04 (C-18), 38.27 (C-1), 37.57 (C-21), 36.73 (C-10), 34.09 (C-2), 33.62 (C-29), 32.05 (C-7), 30.02 (C-20), 27.56 (C-15), 26.41 (C-23), 26.32 (C-27), 25.81 (C-30), 24.04 (C-16), 23.48 (C-11), 21.43 (C-6), 19.47 (C-26), 16.78 (C-24), 15.06 (C-25). ESI-MS (negative-ion mode, m/z): 609.50 ($M^- + 1$), 607.50 ($M^- - 1$).

4.6.11. 22β-Cinnamoyloxy-3-oxo-olean-12-en-28-oic acid (**16**)

Yield: 56.59%, mp: 281–283 °C. Anal. calcd. for $C_{39}H_{52}O_5$ (600.38): %C, 77.96; H, 8.72. Found: %C, 77.99; H, 8.73. IR (KBr, cm^{-1}): 3210 (O–H of COOH), 2950, 2872 (C–H), 1738 (C=O keto), 1699 (C=O), 1632 (C=C). ^1H NMR (400 MHz, $CDCl_3$, δ ppm): 7.4707–7.5108 (1H, d, $J = 16.04$ Hz, C-3′-H), 7.3828–7.4063 (2H, m, C-5′ & C-9′-Ar-H), 7.3229–7.3530 (3H, m, C-6′, C-8′ & C-7′-Ar-H), 6.1513–6.1914 (1H, d, $J = 16.04$ Hz, C-2′-Ar-H), 5.4020–5.4190 (1H, t, $J = 3.40$ Hz, C-12-H), 5.0958–5.1106 (1H, t, $J = 2.96$ Hz, C-22-H), 3.1014–3.1460 (1H, dd, $J = 13.84$, 4.20 Hz, C-18-H), 2.5140–2.5996 (1H, m, C-2-Ha), 2.3373–2.4024 (1H, m, C-2-Hb), 1.1825 (3H, s, CH_3), 1.0890 (3H, s, CH_3), 1.0422 (3H, s, CH_3), 1.0372 (3H, s, CH_3), 1.0086 (3H, s, CH_3), 0.8936 (3H, s, CH_3), 0.8448 (3H, s, CH_3). ^{13}C NMR (100 MHz, $CDCl_3$, δ ppm): 218.03 (C-3), 180.44 (C-28), 165.56 (C-1′), 144.94 (C-3′), 143.05 (C-13), 134.33 (C-4′), 130.74 (C-7′), 128.94 (C-6′ & C-8′), 128.36 (C-5′ & C-9′), 122.57 (C-12), 118.10 (C-2′), 76.52 (C-

22), 55.32 (C-5), 50.82 (C-17), 47.47 (C-9), 46.90 (C-4), 45.94 (C-19), 42.08 (C-14), 39.28 (C-8), 39.16 (C-18), 38.46 (C-1), 37.73 (C-21), 36.77 (C-10), 34.16 (C-2), 33.69 (C-29), 32.18 (C-7), 30.10 (C-20), 27.64 (C-15), 26.45 (C-23), 26.34 (C-27), 25.79 (C-30), 24.01 (C-16), 23.57 (C-11), 21.10 (C-6), 19.54 (C-26), 16.69 (C-24), 15.12 (C-25). ESI-MS (negative-ion mode, *m*/*z*): 599.60 (M^-).

4.7. Synthesis of 3β,22β-dihydroxy-olean-12-en-28-oic acid (**17**)

1 mmol (470.68 mg) of compound **5** was stirred with 1 mmol (37.83 mg) of sodium borohydride in 50 ml solution of methanol (25 ml) and tetrahydrofuran (25 ml) for 7 h (Scheme 2). After completion of reaction, dilute HCl solution was added to the reaction mixture to quench the $NaBH_4$. The organic solvents were removed under reduced pressure and precipitated product was extracted with DCM. The solvent was removed under reduced pressure to afford a compound **17**, which was further purified by using column chromatography (silica gel of 100–200 mesh and gradient mobile phase of hexane–ethyl acetate).

4.7.1. 3β,22β-Dihydroxy-olean-12-en-28-oic acid (**17**)

Yield: 87.79%, mp: 282–284 °C. Anal. calcd. for $C_{30}H_{48}O_4$ (472.36): %C, 76.23; H, 10.24. Found: %C, 76.29; H, 10.23. IR (KBr, cm^{-1}): 3435.07 (O–H), 2948.50, 2876.33 (C–H), 1705.76 (C=O), 1648.59 (C=C). ^1H NMR (400 MHz, $CDCl_3$ + DMSO-d_6 mixture, δ ppm): 11.4773 (1H, s (br), C-28-H (COOH)), 5.2267–5.2441 (1H, t, J = 2.48 Hz, C-12-H), 4.1543 (1H, s (br), C-22-OH), 3.7499–3.7654 (1H, t, J = 3.10 Hz, C-22-H), 3.5768 (1H, s (br), C-3-OH), 3.0544–3.0934 (1H, t, J = 7.80 Hz, C-3-H), 2.9195–2.9626 (1H, dd, J = 13.84, 3.56 Hz, C-18-H), 1.1270 (3H, s, CH_3), 1.0925 (3H, s, CH_3), 0.9397 (3H, s, CH_3), 0.8953 (3H, s, CH_3), 0.8513 (3H, s, CH_3), 0.7982 (3H, s, CH_3), 0.7250 (3H, s, CH_3). ^{13}C NMR (100 MHz, $CDCl_3$ + DMSO-d_6 mixture, δ ppm): 176.23 (C-28), 143.82 (C-13), 120.96 (C-12), 77.16 (C-3), 72.70 (C-22), 54.80 (C-5), 51.00 (C-17), 47.10 (C-9), 46.06 (C-19), 41.63 (C-14), 41.11 (C-8), 38.80 (C-4), 38.30 (C-18), 38.10 (C-1), 37.93 (C-21), 36.52 (C-10), 33.71 (C-29), 32.42 (C-7), 29.79 (C-20), 27.96 (C-2), 27.32 (C-15), 27.06 (C-23), 26.80 (C-27), 25.38 (C-30), 23.89 (C-16), 22.90 (C-11), 17.90 (C-6), 16.69 (C-26), 15.63 (C-24), 15.03 (C-25). ESI-MS (negative-ion mode, *m*/*z*): 472.30 (M^-) 471.20 ($M^- - 1$).

4.8. Synthesis of 3β,22β-diacetoyloxy-olean-12-en-28-oic acid (**18**)

Compound **17** (1 mmol, 472.70 mg) and acetyl chloride (3 mmol, 213.30 μl) were refluxed in pyridine in the presence of 4-DMAP for 10 h at 92–95 °C (Scheme 2). At the end of reaction 10% HCl solution was added to the reaction mixture and precipitated product was extracted with DCM. The product was washed further three times with 10% HCl solution (100 ml × 3) and purified by using column chromatography (silica gel: 100–200 mesh) in a gradient mobile phase of hexane–ethyl acetate.

4.8.1. 3β,22β-Diacetoyloxy-olean-12-en-28-oic acid (**18**)

Yield: 59.25%, mp: 301–303 °C. Anal. calcd. for $C_{34}H_{52}O_6$ (556.38): %C, 73.34; H, 9.41. Found: %C, 73.36; H, 9.40. IR (KBr, cm^{-1}): 3355.26 (O–H of COOH), 2990.34, 2950.25, 2923.26, 2876.39, 2847.49 (C–H), 1731.60 (C=O ester). ^1H NMR (400 MHz, $CDCl_3$, δ ppm): 5.3430–5.3599 (1H, t, J = 3.38 Hz, C-12-H), 5.0028–5.0172 (1H, t, J = 3.88 Hz, C-22-H), 4.4800–4.5196 (1H, t, J = 7.92 Hz, C-3-H), 2.9854–3.0298 (1H, dd, J = 13.76, 4.00 Hz, C-18-H), 2.0498 (3H, s, C-2′-H), 1.9411 (3H, s, C-2″-H), 1.1530 (3H, s, CH_3), 1.0225 (3H, s, CH_3), 0.9472 (3H, s, CH_3), 0.8944 (3H, s, CH_3), 0.8693 (3H, s, CH_3), 0.8606 (3H, s, CH_3), 0.7650 (3H, s, CH_3). ^{13}C NMR (100 MHz, $CDCl_3$, δ ppm): 180.23 (C-28), 171.08 (C-1′), 169.70 (C-1″), 142.86 (C-13), 122.71 (C-12), 80.85 (C-3), 76.14 (C-22), 55.25 (C-5), 50.56 (C-17), 47.52 (C-9), 45.76 (C-19), 41.80 (C-14), 39.24 (C-8), 38.14 (C-18), 38.10 (C-1), 37.68 (C-4), 37.68 (C-21), 36.94 (C-10), 33.69 (C-29), 32.56 (C-7), 30.01 (C-20), 28.02 (C-15), 27.56 (C-23), 26.29 (C-27), 25.86 (C-30), 23.91 (C-16), 23.50 (C-11), 23.44 (C-2), 21.31 (C-2′), 21.10 (C-4′), 18.09 (C-6), 17.05 (C-26), 16.67 (C-24), 15.49 (C-25). ESI-MS (negative-ion mode, *m*/*z*): 556.20 (M^-), 555.20 ($M^- - 1$).

4.9. Synthesis of methyl 22β-hydroxy-3-oxo-olean-12-en-28-ate (**19**)

Compound **5** (1 mmol, 470.68 mg) was refluxed with potassium carbonate (3 mmol, 414.61 mg) in acetone for 1 h. After that dimethyl sulfate (2 mmol, 189.66 μl) was added to the reaction mixture and refluxing was continued for another 11 h (Scheme 2). After completion of reaction, acetone was removed under reduced pressure, reaction mixture was poured into water, and precipitated product was extracted with DCM. Organic solvent was removed in rotary evaporator and crude product was chromatographed over silica gel (100–200 mesh) and eluted with gradient mobile phase of hexane–ethyl acetate to yield a final purified product (**19**).

4.9.1. Methyl 22β-hydroxy-3-oxo-olean-12-en-28-ate (**19**)

Yield: 72.00%, mp: 190–192 °C. Anal. calcd. for $C_{31}H_{48}O_4$ (484.36): %C, 76.82; H, 9.98. Found: %C, 76.83; H, 9.96. IR (KBr, cm^{-1}): 3518 (O–H), 2945 (C–H), 1729 (C=O keto), 1708 (C=O ester). ^1H NMR (400 MHz, $CDCl_3$, δ ppm): 5.3678–5.3843 (1H, t, J = 3.30 Hz, C-12-H), 3.8837–3.8989 (1H, t, J = 3.04 Hz, C-22-H), 3.6702 (3H, s, C-31-H), 3.0396–3.0843 (1H, dd, J = 13.84, 4.04 Hz, C-18-H), 2.5138–2.5995 (1H, m, C-2-Ha), 2.3312–2.3962 (1H, m, C-2-Hb), 1.1555 (3H, s, CH_3), 1.1262 (3H, s, CH_3), 1.0862 (3H, s, CH_3), 1.0628 (3H, s, CH_3), 1.0473 (3H, s, CH_3), 0.8997 (3H, s, CH_3), 0.8244 (3H, s, CH_3). ^{13}C NMR (100 MHz, $CDCl_3$, δ ppm): 217.83 (C-3), 176.14 (C-28), 143.43 (C-13), 122.19 (C-12), 74.62 (C-22), 55.33 (C-5), 52.43 (C-31), 51.58 (C-17), 47.46 (C-9), 46.87 (C-4), 45.97 (C-19), 42.11 (C-14), 41.39 (C-8), 39.27 (C-1), 39.19 (C-18), 38.26 (C-21), 36.75 (C-10), 34.18 (C-2), 33.92 (C-29), 32.21 (C-7), 30.15 (C-20), 27.79 (C-15), 27.20 (C-23), 26.41 (C-27), 25.74 (C-30), 24.49 (C-16), 23.55 (C-11), 21.50 (C-6), 19.57 (C-26), 16.72 (C-24), 15.09 (C-25). ESI-MS (*m*/*z*): 507.50 $(M + Na)^+$, 991.90 $(2M + Na)^+$.

4.10. Synthesis of methyl 3β,22β-dihydroxy-olean-12-en-28-ate (**20**)

Equimolar amount of compound **19** (1 mmol, 484.71 mg) and sodium borohydride (1 mmol, 37.83 mg) was stirred in a 50 ml solution of methanol–tetrahydrofuran (25 ml MeOH + 25 ml THF) for 7 h (Scheme 2). At the end of reaction, sodium borohydride remained was quenched with dilute HCl solution. Organic solvents were removed in rotary evaporator and precipitated product was extracted with DCM. The DCM was removed under reduced pressure and crude product was further purified with the help of column chromatography (silica gel: 100–200 mesh) using gradient mobile phase of hexane–ethyl acetate to give a final purified product (**20**).

4.10.1. Methyl 3β,22β-dihydroxy-olean-12-en-28-ate (**20**)

Yield: 86.70%, mp: 179–180 °C. Anal. calcd. for $C_{31}H_{50}O_4$ (486.37): %C, 76.50; H, 10.35. Found: %C, 76.47; H, 10.33. IR (KBr, cm^{-1}): 3566.56 (O–H), 3368.50 (O–H), 3270.80 (O–H of COOH), 2949.35, 2931.00, 2872.49 (C–H), 1711.48 (C=O), 1565.60 (C=C). ^1H NMR (400 MHz, $CDCl_3$, δ ppm): 5.3429–5.3608 (1H, t, J = 3.58 Hz, C-12-H), 3.8716–3.8883 (1H, t, J = 3.84 Hz, C-22-H), 3.6632 (3H, s, C-31-H), 3.1955–3.2352 (1H, dd, J = 11.36, 5.00 Hz, C-3-H), 3.0220–3.0672 (1H, dd, J = 13.88, 4.20 Hz, C-18-H), 1.1420 (3H, s, CH_3), 1.1216 (3H, s, CH_3), 0.9877 (3H, s, CH_3), 0.9221 (3H, s,

CH_3), 0.8978 (3H, s, CH_3), 0.7835 (3H, s, CH_3), 0.7667 (3H, s, CH_3). ^{13}C NMR (100 MHz, $CDCl_3$, δ ppm): 176.21 (C-28), 143.33 (C-13), 122.44 (C-12), 78.99 (C-3), 74.70 (C-22), 55.22 (C-5), 52.44 (C-31), 51.55 (C-17), 47.62 (C-9), 46.02 (C-19), 42.00 (C-14), 41.38 (C-8), 39.29 (C-18), 38.75 (C-4), 38.48 (C-1), 38.18 (C-21), 37.02 (C-10), 33.91 (C-29), 32.69 (C-7), 30.14 (C-20), 28.09 (C-2), 27.79 (C-15), 27.21 (C-23), 27.18 (C-27), 25.85 (C-30), 24.53 (C-16), 23.46 (C-11), 18.32 (C-6), 16.80 (C-26), 15.58 (C-24), 15.38 (C-25). ESI-MS (m/z): 509.40 $(M + Na)^+$.

4.11. Synthesis of 3β-hydroxylimino-substituted 22β-angeloyloxy/22β-senecioyloxy-olean-12-en-28-oic acids (**21**–**22**)

1 mmol (552.78 mg) of lantadene (**1**, **2**) was refluxed with 10 equivalent of hydroxylamine hydrochloride (10 mmol, 694.90 mg) in pyridine at 92–95 °C for 8 h (Scheme 2). The reaction mixture was poured into 10% HCl solution and product was extracted with DCM and washed further three times with 10% HCl solution (100 ml × 3). The organic solvent was removed under reduced pressure to dryness and crude product obtained was subjected to column chromatography using silica gel (100–200 mesh) and gradient mobile phase of hexane–ethyl acetate to yield a final purified product (**21**–**22**).

4.11.1. 22β-Angeloyloxy-3-hydroxylimino-olean-12-en-28-oic acid (**21**)

Yield: 59.88%, mp: 235–236 °C. Anal. calcd. for $C_{35}H_{53}NO_5$ (567.39): %C, 74.04; H, 9.41. Found: %C, 74.00; H, 9.40. IR (KBr, cm^{-1}): 3271.11 (O–H), 2951.50 (C–H), 1718.30 (C=O), 1647.24 (C=C). ^1H NMR (400 MHz, $CDCl_3$ + DMSO-d_6 mixture, δ ppm): 11.7341 (1H, s (br), C-28-H (COOH)), 5.9792–6.0290 (1H, m, C-33-H), 5.3471–5.3645 (1H, t, J = 3.48 Hz, C-12-H), 5.0170–5.0317 (1H, t, J = 2.94 Hz, C-22-H), 2.2019–2.2610 (1H, m, C-2-Ha), 2.0594–2.1419 (1H, m, C-2-Hb), 1.1498 (3H, s, CH_3), 1.0272 (3H, s, CH_3), 1.0189 (6H, s, 2× CH_3), 1.0096 (3H, s, CH_3), 0.8932 (3H, s, CH_3), 0.8598 (3H, s, CH_3). ^{13}C NMR (100 MHz, $CDCl_3$ + DMSO-d_6 mixture, δ ppm): 175.35 (C-28), 165.77 (C-31), 164.22 (C-3), 143.11 (C-13), 137.35 (C-33), 127.57 (C-32), 121.46 (C-12), 75.60 (C-22), 55.29 (C-5), 49.65 (C-17), 46.60 (C-9), 45.53 (C-19), 41.51 (C-14), 39.50 (C-4), 38.81 (C-8), 38.12 (C-18), 37.79 (C-1), 37.39 (C-21), 36.50 (C-10), 33.31 (C-29), 31.99 (C-7), 29.55 (C-20), 27.18 (C-15), 27.06 (C-23), 25.76 (C-27), 25.27 (C-30), 23.64 (C-16), 23.10 (C-2), 22.89 (C-11), 20.07 (C-6), 18.51 (C-35), 16.42 (C-26), 16.34 (C-34), 15.14 (C-24), 14.40 (C-25). ESI-MS (negative-ion mode, m/z): 567.30 (M^-), 566.30 ($M^- - 1$).

4.11.2. 22β-Senecioyloxy-3-hydroxylimino-olean-12-en-28-oic acid (**22**)

Yield: 59.53%, mp: 231–232 °C. Anal. calcd. for $C_{35}H_{53}NO_5$ (567.39): %C, 74.04; H, 9.41. Found: %C, 74.10; H, 9.42. IR (KBr, cm^{-1}): 3256.38 (O–H), 2953.32, 2926.07, 2859.85 (C–H), 1738.33 (C=O), 1720.33 (C=O), 1647.17 (C=C). ^1H NMR (400 MHz, $CDCl_3$ + DMSO-d_6 mixture, δ ppm): 11.7373 (1H, s (br), C-28-H (COOH)), 5.5564 (1H, s, C-32-H), 5.3506 (1H, s, C-12-H), 5.0073–5.0238 (1H, t, J = 3.30 Hz, C-22-H), 2.2105–2.2568 (1H, m, C-2-Ha), 2.0545–2.1524 (1H, m, C-2-Hb), 1.1478 (3H, s, CH_3), 1.0251 (3H, s, CH_3), 1.0167 (6H, s, 2× CH_3), 1.0086 (3H, s, CH_3), 0.8872 (3H, s, CH_3), 0.8578 (3H, s, CH_3). ^{13}C NMR (100 MHz, $CDCl_3$ + DMSO-d_6 mixture, δ ppm): 181.24 (C-28), 165.73 (C-31), 164.08 (C-3), 156.41 (C-33), 143.12 (C-13), 121.49 (C-12), 116.77 (C-32), 75.59 (C-22), 55.28 (C-5), 49.52 (C-17), 46.59 (C-9), 45.55 (C-19), 41.52 (C-14), 39.48 (C-4), 38.81 (C-8), 38.00 (C-18), 37.80 (C-1), 37.40 (C-21), 36.51 (C-10), 33.33 (C-29), 32.00 (C-7), 29.56 (C-20), 27.21 (C-15), 27.06 (C-23), 26.00 (C-35), 25.77 (C-27), 25.27 (C-30), 23.57 (C-16), 23.12 (C-2), 22.89 (C-11), 20.08 (C-6), 16.39 (C-26), 16.33 (C-34), 15.15 (C-24), 14.43 (C-25). ESI-MS (negative-ion mode, m/z): 568.30 ($M^- + 1$).

4.12. In vitro cell culturing and cytotoxicity assay

The A549 lung cancer cell line was obtained from American Type Culture Collection (ATCC, USA) and was grown in RPMI medium supplemented with 5% fetal bovine serum and 1% penicillin-streptomycin (Gibco, Invitrogen, USA). The A549 (4000 cells/well) were seeded into 96-well plates and incubated overnight for cell attachment. For treatment, compounds were added at concentrations ranging from 0.01 to 100 μmol and incubated for 48 h. At the end of incubation, 20 μl/well of 5 mg/ml 3-(4,5-dimethythiazol-2-yl)-2,5-diphenyltetrazolium bromide (MTT) (Amresco, USA) was added and cells were further incubated for 4 h. Supernatant was then removed and the purple formazan which has formed was dissolved using 100 μl of DMSO (Fisher Scientific, UK). Absorbance was read at 570 nm using Spectra Max M4 microplate reader (Molecular Devices Inc., US).

4.13. In vitro inhibition of TNF-α-induced NF-κB activation in A549 lung cells

The A549 cells were cultured in 12-well plates and transiently co-transfected with 0.2 μg of a pNF-κB-Luc vector (Stratagene, La Jolla, CA) and 0.2 μg of pSV-β-galactosidase dissolved in 3 μl lipofectamine™ or lipofectamine™ 2000 (Invitrogen, Carlsbad, CA) as the internal control. The plasmids were transfected according to the manufacturer's instructions. After 6 h, the medium was changed and cells were cultured for 6 h. Cells were then treated with TNF-α (15 ng/ml) and test compounds simultaneously for 7 h. The A549 cells treated with TNF-α alone served as positive controls, while cells without TNF-α treatment served as negative controls. Luciferase activities from these cells were then measured by using the Bright-Glo Luciferase Assay kit from Promega (Madison, WI), following the manufacturer's protocol. The relative NF-κB activities of the cells treated by test compounds were obtained as the ratio of its luciferase activity to that from the positive controls, both of which have been corrected with background (signals from negative controls) and cell viability. In these experimental conditions, none of the test compounds induced significant toxicity to A549 cells (<5% reduction of cell viability). The IC_{50} of each fraction was determined by fitting the relative NF-κB activity to the drug concentration by using a sigmoidal dose–response model of varied slope in GraphPad Prism 6. The IC_{50} reported herein is the average of at least three replicates.

4.14. In vitro phosphorylation assay

The cDNA encoding human IKKβ was isolated by PCR with primers containing sequences encoding a FLAG tag in the carboxy-terminal region and subcloned into an insect cell expression vector, pFASTBAC1 (Invitrogen, U.S.A.). The Sf21 cells were infected with IKKβ recombinant baculovirus and cultured at 28 °C for 72 h. The cells were lysed and FLAG-tagged IKKβ protein was purified by affinity chromatography using anti-FLAG M2 affinity gel (Sigma, U.S.A.). The kinase reaction of purified human IKKβ was performed at room temperature for 1 h in kinase reaction buffer (25 mmol/l HEPES, pH 7.5, 10 mmol/l magnesium acetate, 1 mmol dithiothreitol, 0.01% bovine serum albumin, 0.01% Tween20) containing 500 nmol ATP, and bacterially expressed GST-IκBα, and then terminated by adding the same volume of Kinase-Glo™ reagent (Promega, U.S.A.). After incubating at room temperature for 10 min the luminescent signal correlated with the amount of ATP

remaining in solution following the reaction was measured by Wallac Arvo HTS multilabel counter (PerkinElmer, U.S.A.).

4.15. Predicting binding mode of lead ester congener **13** to IKKβ

Crystal structure of IKKβ was downloaded from Protein Data Bank (PDB ID: 3QA8) [16]. Structures of ligands in PDB format were prepared using CS ChemDraw Ultra 8.0. Molecular docking study was performed using AutoDock tools 1.5.4. Protein was firstly prepared by adding polar hydrogen atoms at pH 7.4 followed by assigning of the Gasteiger charges. Nonpolar hydrogens were merged and partial charges to their parent carbon atoms were added. The search space was identified as a cubic box with dimensions 40 Å × 40 Å × 40 Å and center $x = -20$, $y = -15$, $z = 30$. The Lamarckian genetic algorithm (LGA) was applied to explore conformers with lowest binding energy. Results of molecular docking analysis were obtained as estimated free energy of binding in kcal/mol (docking score).

4.16. HPLC analysis

Compounds were studied for chemical and metabolic stability, and chromatographic purity using reversed-phase high-performance liquid chromatography (HPLC). The isocratic solvent systems comprising of methanol–acetonitrile–water–acetic acid (68:20:12:0.01) and methanol–acetonitrile–water–acetic acid (68:22:10:0.01) were used as mobile phase in HPLC studies. The mobile phase constituents for HPLC analysis were mixed (v/v) and filtered through 0.45 μm Millipore membrane filter. The injection volume was 10 μl and flow-rate was kept 1 ml/min. Peak areas showed excellent reproducibility with relative standard deviation of 0.5%.

4.16.1. In vitro stability of lead ester congeners in simulated gastric fluid of pH 2

Lead ester congeners **12** and **13** were studied for their *in vitro* stability in simulated gastric fluid using HCl buffer of pH 2 at 37 °C. To start the reaction, 200 μl stock solution of compound (5 mg/ml in THF) was added to the 1.80 ml of HCl buffer of pH 2 in screw-capped glass vials. Reaction mixture was incubated on a water bath at constant temperature and samples (200 μl) were withdrawn at appropriate time intervals, diluted with 800 μl ACN, and analyzed using HPLC. The percentage of ester congener remaining was calculated by using formula: % remaining = (peak area at respective time (min)/peak area at 0 min) × 100.

4.16.2. In vitro physiological stability of lead ester congeners in human plasma

Lead ester congeners **12** and **13** were studied for their enzymatic hydrolysis in 80% human plasma diluted with isotonic phosphate buffer of pH 7.4. The reaction was induced by adding 50 μl of stock solution of compound (5 mg/ml in THF) to the 450 μl of diluted plasma. The solution was incubated on a water bath at 37 °C. The samples (50 μl) were withdrawn at appropriate time intervals and added to the 1950 μl of ACN. Sample mixture was then centrifuged for 5 min at 7000 rpm and supernatant was used for HPLC analysis. The percentage of ester congener remaining was calculated as: % remaining = (peak area at respective time (min)/peak area at 0 min) × 100.

Conflict of interest

The author(s) confirm that this article content has no conflict of interest.

Acknowledgments

Authors are thankful to Department of Science and Technology, Government of India for financial assistance for this research work. We are also thankful to Sophisticated Analytical Instrumentation Facility (SAIF), Panjab University, Chandigarh, India for spectral analyses.

Appendix A. Supplementary data

Supplementary data related to this article can be found at http://dx.doi.org/10.1016/j.ejmech.2013.12.052.

References

[1] W. Xiao, Advances in NF-kappaB signaling transduction and transcription, Cell. Mol. Immunol. 1 (2004) 425–435.
[2] E. Pikarsky, R.M. Porat, I. Stein, R. Abramovitch, S. Amit, S. Kasem, E. Gutkovich-Pyest, S. Urieli-Shoval, E. Galun, Y. Ben-Neriah, NF-κB functions as a tumour promoter in inflammation-associated cancer, Nature 431 (2004) 461–466.
[3] D.S. Basseres, A.S. Baldwin, Nuclear factor-kappaB and inhibitor of kappaB kinase pathways in oncogenic initiation and progression, Oncogene 25 (2006) 6817–6830.
[4] M. Karin, Nuclear factor-kappaB in cancer development and progression, Nature 441 (2006) 431–436.
[5] F. Li, G. Sethi, Targeting transcription factor NF-kappaB to overcome chemoresistance and radioresistance in cancer therapy, Biochim. Biophys. Acta 1805 (2010) 167–180.
[6] B.K. Bednarski, X. Ding, K. Coombe, A.S. Baldwin, H.J. Kim, Active roles for inhibitory kappaB kinases alpha and beta in nuclear factor-kappaB-mediated chemoresistance to doxorubicin, Mol. Cancer Ther. 7 (2008) 1827–1835.
[7] S.C. Gupta, C. Sundaram, S. Reuter, B.B. Aggarwal, Inhibiting NF-κB activation by small molecules as a therapeutic strategy, Biochim. Biophys. Acta 1799 (2010) 775–787.
[8] J. Kaur, M. Sharma, P.D. Sharma, M.P. Bansal, Chemopreventive activity of lantadenes on two-stage carcinogenesis model in Swiss albino mice: AP-1 (c-jun), NF κB (p65) and p55 expression by ELISA and immunohistochemical localization, Mol. Cell. Biochem. 314 (2008) 1–8.
[9] J. Kaur, M. Sharma, P.D. Sharma, M.P. Bansal, Antitumor activity of lantadenes in DMBA/TPA induced skin tumors in mice: expression of transcription factors, Am. J. Biomed. Sci. 2 (2010) 79–90.
[10] M. Sharma, P.D. Sharma, M.P. Bansal, J. Singh, Lantadene A-induced apoptosis in human leukemia HL-60 cells, Ind. J. Pharmacol. 39 (2007) 140–144.
[11] M. Sharma, P.D. Sharma, M.P. Bansal, Lantadenes and their esters as potential antitumor agents, J. Nat. Prod. 71 (2008) 1222–1227.
[12] N.K. Tailor, H.B. Lee, M. Sharma, Synthesis and *in vitro* anticancer studies of novel C-2 arylidene congeners of lantadenes, Eur. J. Med. Chem. 64 (2013) 285–291.
[13] N.K. Tailor, V. Jaiswal, S.S. Lan, H.B. Lee, M. Sharma, Synthesis, selective cancer cytotoxicity and mechanistic studies of novel analogs of lantadenes, Anti-cancer Agents Med. Chem. 13 (2013) 957–966.
[14] J.A. Schmid, A. Birbach, IkappaB kinase beta (IKKbeta/IKK2/IKBKB) – a key molecule in signaling to the transcription factor NF-kappaB, Cytokine Growth Factor Rev. 19 (2008) 157–165.
[15] S. Ballaz, J.L. Mulshine, The potential contributions of chronic inflammation to lung carcinogenesis, Clin. Lung Cancer 5 (2003) 46–62.
[16] G. Xu, Y.C. Lo, Q. Li, G. Napolitano, X. Wu, X. Jiang, M. Dreano, M. Karin, H. Wu, Crystal structure of inhibitor of κB kinase β, Nature 472 (2011) 325–330.
[17] S.K. Suthar, N. Tailor, H.B. Lee, M. Sharma, Reduced lantadenes A and B: semi-synthetic synthesis, selective cytotoxicity, apoptosis induction and inhibition of NO, TNF-α production in HL-60 cells, Med. Chem. Res. 22 (2013) 3379–3388.